Journal of Solid State Chemistry 185 (2012) 229–237

Contents lists available at SciVerse ScienceDirect

Journal of Solid State Chemistry

journal homepage: www.elsevier.com/locate/jssc

Magnetic behaviour of the $MTbF_6$ fluoroterbates (M=Cd, Ca, Sr, (α/β)-Ba)

M. Josse [a,d], M. El-Ghozzi [a,*], D. Avignant [a], G. André [b], F. Bourée [b], O. Isnard [c]

[a] Laboratoire des Matériaux Inorganiques, UMR 6002 CNRS, Université Blaise Pascal, 63171 Aubière, France
[b] Laboratoire Léon Brillouin, CEA-CNRS, CEA-Saclay, 91191 Gif-sur-Yvette, France
[c] Institut Néel, CNRS/Université Joseph Fourier, UPR2940, 38042 Grenoble, France
[d] CNRS, Université de Bordeaux, ICMCB, Pessac, France

ARTICLE INFO

Article history:
Received 24 June 2011
Received in revised form
3 October 2011
Accepted 17 October 2011
Available online 11 November 2011

Keywords:
Tetravalent terbium
Fluorides
Neutron diffraction
Magnetic structure
Metamagnetism
Superexchange

ABSTRACT

Neutron powder diffraction has been performed on the $MTbF_6$ fluorides (M=Cd, Ca, Sr, (α/β)-Ba). Four of these fluorides (Cd, Ca, Sr, β-Ba) are built of a (pseudo-) tetragonal packing of $[TbF_6]^{2-}$ chains and only differs by the chains relative orientations. Thus this series represents a valuable opportunity to evaluate the Tb^{4+}-Tb^{4+} magnetic interactions. All the compounds displayed antiferromagnetic order (T_N=2.70 K (Cd), 2.15 K (Ca), 2.60 K (Sr), 2.10 K (β-Ba)), except for the α form of $BaTbF_6$. The crystal structure of this latter fluoroterbate has also been investigated by means of high-resolution neutron powder diffraction. From Neutron Powder Diffraction data, $CdTbF_6$ and β-$BaTbF_6$ magnetic structures were determined, together with the metamagnetic behaviour of β-$BaTbF_6$ as a function of an external magnetic field. A tentative phase diagram is then given for β-$BaTbF_6$. Advantage was taken of the polymorphism of the $BaTbF_6$ fluoroterbate to analyse, on the basis of topological parameters such as bond distances and angles, the magnetic behaviour of its α and β forms. It was shown that superexchange interactions are present in β-$BaTbF_6$, and that these interactions may also rule the magnetic behaviour of the other $MTbF_6$ (M=Ca, Sr, Cd) tetravalent terbium fluorides.

1. Introduction

The magnetic properties of paramagnetic lanthanides ions are related to their partially filled 4*f* shell, which is known to have a pronounced internal character. Because of their limited spatial extension and of the screening of the 5*d* and 6*s* shells, 4*f* electrons hardly interact with the electronic shells of neighbouring atoms, especially with other 4*f* electrons. Thus chemical bonding of rare-earths in oxides and fluorides is predominantly ionic, and their magnetism is usually dominated by dipolar interactions, especially in fluorides.

However structural studies of tetravalent terbium fluorides suggest that the singular crystal-chemistry of this class of fluorides (a propensity of the Tb^{4+} ions to adopt an 8-fold coordination) may be influenced by the half-filled 4*f* shell of the Tb^{4+} ion [1,2], i.e. that 4*f* electrons influence the Tb–F chemical bonding in these compounds.

Similarly, the magnetic behaviour of fluoroterbates, studied for many years in our laboratory, tends to demonstrate that non-dipolar interactions occur in these materials and may rule their magnetic behaviour [3–5], as for example, the recent study of the magnetic behaviour of M_2TbF_6 (M=Li, K, Rb) fluorides [6]. In these fluoroterbates incommensurate square-modulated magnetic structures are observed at low temperature (below 2.1 K). The ordering temperature observed have been correlated to the efficiency of the dipolar interactions to relay the frustration induced by the pseudo-hexagonal packing of magnetic $[TbF_6]^{2-}$ chains, while the magnetic behaviour of Li_2TbF_6 suggests non-dipolar interactions in these chains.

To supplement our investigations, in order to bring further evidences of these non-dipolar interactions, we investigated the magnetic behaviour of the $MTbF_6$ (M=Cd, Ca, Sr, (α/β)-Ba) fluorides.

The crystal structures of α and β polymorphs of $BaTbF_6$ were the first, among fluoroterbates, to be determined from single-crystal X-ray diffraction (XRD) [7,8]. $SrTbF_6$ was reported to be isomorphic to β-$BaZrF_6$ [9]. $CaTbF_6$ and $CdTbF_6$ adopt an anti-$KSbF_6$ [2] and are, after Li_2TbF_6 [1], new examples of the singular crystal-chemistry of fluoroterbates. The remarkable feature of the $MTbF_6$ fluorides is that they are all, except α-$BaTbF_6$, built of $[TbF_6]^{2-}$ chains (Fig. 1). These chains adopt different orientation, depending on the size of the associated alkaline earth, yielding different symmetries for the corresponding crystal structure. This series represents a valuable opportunity to evaluate the Tb^{4+}–Tb^{4+} magnetic interactions, due to the homogeneity of the polyhedral frameworks ($[TbF_6]^{2-}$ chains) on one hand, and to the polymorphism of $BaTbF_6$ on the other hand, which should allow more insight the structural parameters influencing the magnetic behaviour of fluoroterbates.

* Corresponding author.
E-mail address: Malika.EL-GHOZZI@univ-bpclermont.fr (M. El-Ghozzi).

0022-4596/$ - see front matter © 2011 Elsevier Inc. All rights reserved.
doi:10.1016/j.jssc.2011.10.030

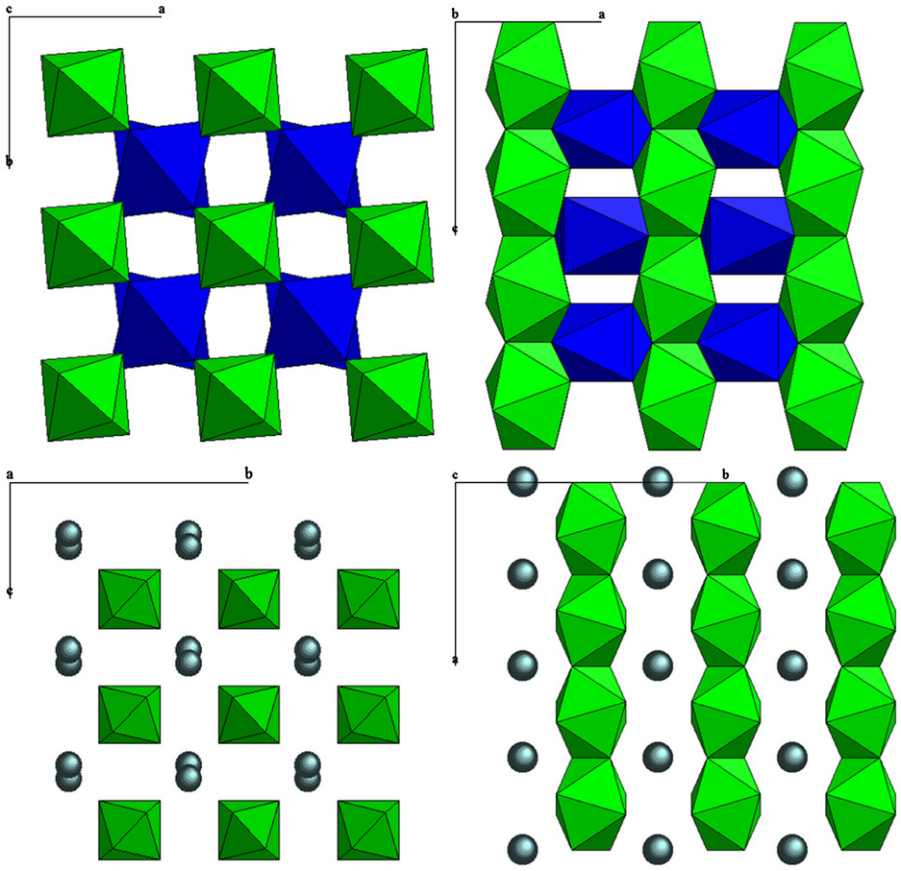

Fig. 1. Crystal structure of $CaTbF_6$ and $CdTbF_6$ viewed along the *c*-axis (top left) and the *b*-axis (top right), Tb^{4+} polyhedra in green, Ca^{2+}/Cd^{2+} polyhedra in blue. Crystal structure of $SrTbF_6$ and β-$BaTbF_6$ viewed along the *a*-axis (bottom left) and the *c*-axis (bottom right), Tb^{4+} polyhedra in green, Sr^{2+}/Ba^{2+} as spheres. (For interpretation of the references to color in this figure legend, the reader is referred to the web version of this article.)

The present work deals with a neutron diffraction study of the magnetic behaviour of the titles compounds. The magnetic structures of $CdTbF_6$ and β-$BaTbF_6$ were determined. The crystal structure of α-$BaTbF_6$ was also investigated by means of high resolution powder neutron diffraction to benefit from the most accurate description of its anionic framework.

The magnetic behaviour in these $MTbF_6$ (M=Cd, Ca, Sr, Ba) compounds will be discussed with respect to crystal-chemical considerations, with a particular focus on the α and β polymorphs of $BaTbF_6$. The nature of the magnetic interactions involved in these fluoroterbates will be investigated.

2. Material and methods

Polycrystalline samples of the title compounds were obtained by heating overnight stoichiometric mixtures of MF_2 (Strem chemicals) (M=Cd, Ca, Sr, Ba) and TbF_4 (prepared by fluorination of Tb_4O_7, (Merck)), under pure fluorine gas, at 500 °C. The samples were then annealed for 12 h at temperatures ranging from 540 to 720 °C.

Neutron powder diffraction patterns were recorded at the Leon Brillouin Laboratory (LLB, Saclay, France) on the two-axis G4.1 diffractometer (λ=2.4266 Å) down to 1.4 K, without any magnetic field, for the determination of the magnetic structure [10], and on the 3T2 high resolution diffractometer (λ=1.2251 Å) at 300 K for the refinement of the crystal structure of α-$BaTbF_6$. It is worth mentioning that all the structural refinements performed were fully consistent with the previously reported crystallographic data [2,4,7,8], and thus confirmed the tetravalent oxidation state of terbium ions in the title compounds. NDP under magnetic field for the β-$BaTbF_6$ fluororterbate were recorded on the super-D2B instrument at the Institut Laue Langevin (ILL, Grenoble). The data were analysed with the FULLPROF program [11], using the magnetic form factor of Gd^{3+} for the magnetic refinements, as this ion is isoelectronic to Tb^{4+} for which no magnetic form factors are available. The dipolar magnetostatic energy of β-$BaTbF_6$ has been obtained using the concept of non-overlapping charges developed by Bertaut [12] to account for the long range character of the dipolar interactions. The results in Section 3.1.3 are for Tb^{4+} magnetic moments equal to 7 μ_B (theoretical value).

3. Results and discussion

3.1. α and β-$BaTbF_6$ fluorides

3.1.1. Nuclear structure

3.1.1.1. ***α–β–$BaTbF_6$:.*** Neutron Powder Diffraction (NPD) patterns were recorded on the G4-1 diffractometer in the temperature range 1.4–5 K. The nuclear structure of β-$BaTbF_6$ at 5 K was refined on the basis of the model determined from single-crystal X-ray diffraction [8], leading to conventional R_{Bragg}=3.0% (Table 1). Refined atomic coordinates, in good agreement with those obtained from single-crystal X-ray data, are presented in Table 2. The crystal structure of β-$BaTbF_6$ is built of infinite $[TbF_6]^{2-}$ linear chains arising from $[TbF_8]^{4-}$ polyhedra sharing opposite and almost orthogonal edges. These chains adopt a

pseudo-tetragonal packing and are linked by the Ba^{2+} ions, which are surrounded by four $[TbF_6]^{2-}$ chains. In this structure, the $[TbF_6]^{2-}$ chains are rigorously linear (Tb–Tb–Tb angles are equal to 180° in the chains).

Table 1
Characteristics of the neutron powder diffraction Rietveld refinement of α-$BaTbF_6$ (300 K) and β-$BaTbF_6$ (5K) nuclear structures.

	β-$BaTbF_6$ (nuclear, G4-1)	α-$BaTbF_6$ (nuclear, 3T2)
System and space group	Orthorhombic *Cmma* (no. 67)	Triclinic $P\bar{1}$ (no. 2)
Refined cell parameters: (Å and deg.)	a=7.760(1), b=11.600(1), c=5.485(1)	a=7.348(1), b=8.448(1), c=8.675(1)
	Z=4	α=101.62(1), β=96.83(1), γ=114.65(1) Z=4
Wavelength (Å)	2.4266	1.2251
2θ range/step	8–88° × 0.1	6–125.7° × 0.05
Number of independent reflections	30	3190
Number of intensity dependent parameters	11	48
Conventional rietveld reliability factor (%)		
R_p	11.3	8.06
R_{wp}	10.7	7.97
R_{Bragg}	2.98	4.02
R_F	3.04	2.06
χ^2	8.25	1.78

Table 2
Atomic positions refined at 5 K (from G4-1 data) for β-$BaTbF_6$.

Atom	X	Y	Z
Ba	0	1/4	0.4436(1)
Tb	1/4	0	0
F(1)	0	0.4300(4)	0.1557(8)
F(2)	0.3060(4)	0.3719(3)	0.2541(6)

*3.1.1.2. **b–α-BaTbF$_6$**:.* The crystal structure of α-$BaTbF_6$ has been previously determined from single-crystal X-ray diffraction [7], but the low symmetry (space group $P\bar{1}$) lead us to record a NPD at 300 K, using thermal neutron (λ=1.2251 Å), on the high resolution diffractometer 3T2, in order to confirm the positional parameters of the fluorine atoms. As shown by Fig. 2, the Rietveld refinement unambiguously confirmed the triclinic symmetry, with R_{Bragg}=4.0% (Table 1). The refined atomic coordinates gathered in Table 3 show the good agreement between X-ray and neutron data. The crystal structure of α-$BaTbF_6$ is based on tetrameric units $[Tb_4F_{26}]^{10-}$ built by corner sharing between $[Tb_2F_{14}]^{6-}$ dimers, themselves built of $[TbF_8]^{4-}$ polyhedra sharing an edge, as displayed by Fig. 3(a). These $[Tb_4F_{26}]^{10-}$ tetramers are further linked together by two common corners, leading to the formation of corrugated layers of $[TbF_6]^{2-}$ formula that expand along the a and b-axes. The Ba^{2+} ions lie between these corrugated layers.

3.1.2. Magnetic studies

*3.1.2.1. **α–β-BaTbF$_6$**.* **(i) *Zero field study***

At low temperature, several purely magnetic Bragg peaks appear in the β-$BaTbF_6$ NPD diagram, that can be indexed in the orthorhombic (a b 2c) magnetic unit cell, with h even, k and l odd indices. As a direct consequence of these selection rules, two magnetic moments separated by [1/2 0 0] in the crystal unit cell are identical, and opposite when they are separated either by [1/2 1/2 0] or [0 0 1]. The resulting magnetic structure is then antiferromagnetic, with ferromagnetic $[TbF_6]^{2-}$ chains, and antiferromagnetic coupling between neighbouring $[TbF_6]^{2-}$ chains. The thermal variation of the intensity of the most intense magnetic Bragg peak (Fig. 4) lead to T_N=2.1(1) K.

Let us note that this magnetic structure can also be described using the commensurate propagation vector **k**=(0 1 1/2). Bertaut's representation analysis [13] for *Cmma* space group, **k**=(0 1 1/2) propagation vector and (4a) Wyckoff position, leads first to an 8-dimensional $G_{\mathbf{k}}$ group (all the rotational symmetry elements of the space group *Cmma* (D_{2h}^{21}) leave **k** invariant) and then to eight one-dimensional irreducible representations for $G_{\mathbf{k}}$ (Table 4). For the (4a) Wyckoff position, only two Tb^{4+} in the crystal unit-cell

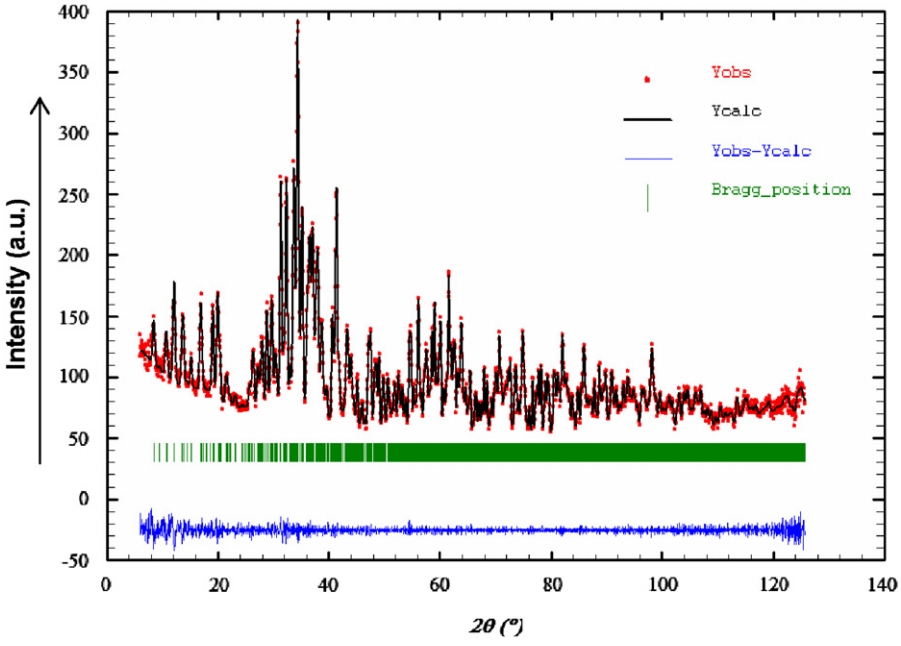

Fig. 2. Rietveld plot for the refinement of α-$BaTbF_6$ nuclear structure at 300 K (3T2 data).

Table 3
Atomic positions (300 K) refined from single-crystal XRD data (top) [7] and from high resolution neutron powder diffraction data (bottom, in italic) for α-$BaTbF_6$.

Atom	X	Y	Z	B (Å²)
Tb1	0.18367(8)	0.25951(7)	0.28111(7)	0.430(8)
	0.1836(6)	*0.2579(5)*	*0.2815(5)*	*0.51(4)*
Tb2	0.22918(8)	0.78338(7)	0.06120(7)	0.387(7)
	0.2286(5)	*0.7823(5)*	*0.0615(4)*	*0.51(4)*
Ba1	0.2988(1)	0.31428(9)	0.76950(9)	0.66(1)
	0.2971(8)	*0.3130(8)*	*0.7691(6)*	*0.62(6)*
Ba2	0.7072(1)	0.2311(1)	0.45645(9)	0.72(1)
	0.7067(8)	*0.2294(7)*	*0.4559(6)*	*0.62(6)*
F1	0.095(1)	0.236(1)	0.027(1)	1.0(1)
	0.0975(8)	*0.2364(7)*	*0.0258(7)*	*1.07(3)*
F2	0.119(1)	0.383(1)	0.496(1)	1.0(1)
	0.1171(7)	*0.3833(7)*	*0.4956(1)*	*1.07(3)*
F3	1/2	0	0	1.3(2)
	1/2	*0*	*0*	*1.07(3)*
F4	0.087 (1)	0.754(1)	0.258(1)	1.2(1)
	0.0877(8)	*0.7542(7)*	*0.2589(6)*	*1.07(3)*
F5	0.292(1)	0.534(1)	0.288(1)	1.1(1)
	0.2928(8)	*0.5355(6)*	*0.2873(6)*	*1.07(3)*
F6	0	1/2	0	1.2(2)
	0	*1/2*	*0*	1.07(3)
F7	0.527(1)	0.108(1)	0.726(1)	1.0(1)
	0.5262(8)	*0.1078(7)*	*0.7247(7)*	*1.07(3)*
F8	0.396(1)	0.638(1)	0.001(1)	1.1(1)
	0.3924(8)	*0.6350(7)*	*0.0011(6)*	*1.07(3)*
F9	0.310(1)	0.177(1)	0.469(1)	1.2(1)
	0.3120(8)	*0.1772(7)*	*0.4693(6)*	*1.07(3)*
F10	0.869(1)	0.284(1)	0.199(1)	1.1(1)
	0.8692(9)	*0.2830(8)*	*0.1978(6)*	*1.07(3)*
F11	0.082(1)	0.960(1)	0.703(1)	1.4(2)
	0.0814(8)	*0.9612(7)*	*0.7018(6)*	*1.07(3)*
F12	0.236(1)	0.041 (1)	0.145(1)	1.2(1)
	0.2350(8)	*0.04047(7)*	*0.14688(7)*	*1.07(3)*
F13	0.497(1)	0.6230(1)	0.702(16)	1.4(2)
	0.4943(8)	*0.6296(7)*	*0.7029(6)*	*1.07(3)*

have to be characterised from a magnetic point of view: Tb1 in [1/4 0 0] and Tb2 in [3/4 0 0]. From their magnetic moments, S1 and S2 respectively, one immediately gets the magnetic moments for all Tb^{4+} ions in the magnetic ($a\,b\,2c$) unit-cell, as [1/2 1/2 0] and [0 0 1] translations are associated to a change of sign for the magnetic moment components. The magnetic representation Γ is associated to 6×6 matrices, characteristic of the transformations of the spin components of Tb1 and Tb2 by $G_{\mathbf{k}}$ symmetry elements (Table of Γ characters: 6 2 2 −2 0 0 0 0). This 6-dimensional representation can be reduced as $\Gamma=\tau_1+\tau_2+\tau_3+\tau_4+\tau_5+\tau_6$. The basic vectors associated with each representation appearing in Γ correspond to six possible magnetic structures, namely three ferromagnetic $[TbF_6]^{2-}$ chains and three antiferromagnetic $[TbF_6]^{2-}$ chains, the Tb^{4+} magnetic moments within a chain being parallel either to the **a** or **b** or **c** axis (Table 5). Let us recall that the resulting magnetic structure for the 8 Tb^{4+} in the magnetic unit cell is antiferromagnetic, whatever τ_{1-6}, as [1/2 1/2 0] and [0 0 1] translations are always associated to a change of sign for the magnetic moment components from one chain to the neighbouring ones. The best agreement between observed and calculated NPD diagrams for the magnetic structures described above [τ_i, $i=1$–6] is unambiguously obtained for τ_1, a structure based on ferromagnetic arrangement of Tb^{4+} magnetic moments within the $[TbF_6]^{2-}$ chains and antiferromagnetic interactions between these chains (Table 6 and Fig. 5). Each Tb^{4+} magnetic moment is directed along the *a*-axis of the crystal structure, *i.e.* along the direction of the $[TbF_6]^{2-}$ chains, and equal to 6.68(3) μ_B, as compared to the 7 μ_B theoretical $g_J J$ value (Table 4). This magnetic structure can be described by the magnetic group C_Imma.

(ii) Neutron diffraction under magnetic field

In order to evaluate the stability of the antiferromagnetic structure under external magnetic field, we undertook a neutron diffraction study under magnetic field (H). As powder samples may exhibit superparamagnetic behaviour, we prepared sintered pellets (to avoid grain reorientation) of β-$BaTbF_6$ that were broken into millimetric parts (to avoid preferred orientation due to pellet texturation) and then placed in the 8 mm diameter cylindrical sample holder (applied magnetic field was parallel to the sample holder axis).

NPD data obtained in zero-field cooled process confirmed the antiferromagnetic transition previously observed at $T_N=2.1$ K (see Fig. 4).

The progressive application of magnetic field at 1.4 K (in the antiferromagnetic state) first induced a reduction of the intensity of antiferromagnetic contributions in the NDP. Around 0.15 T, small contributions associated with the onset of ferromagnetic order were observed, and grew with increase of the applied magnetic field. At 1 T a small amount of the antiferromagnetic phase was still present, while at 4 T the sample was completely ferromagnetic (Fig. 6).

The same procedure repeated at higher temperatures did not reveal significant changes in the onset of this magnetic transition. It is worth to note that the ferromagnetic ordering could be stabilised above T_N by applying magnetic field, for example at $T=2.34$ K with $H=1$ T. After heating the sample up to 20 K, the antiferromagnetic ordering could be observed again below 2.1 K after a zero field cooling.

This experience both confirmed the zero field antiferromagnetic ordering in β-$BaTbF_6$ and revealed its metamagnetic behaviour, which originates from the weakness of interchains magnetic interactions, with Tb–Tb distances exceeding 5.5 Å.

A tentative H–T magnetic phase diagram (Fig. 7) has been built from our observation of the evolution of β-$BaTbF_6$ magnetic structure under magnetic field.

3.1.2.2. ***b–α-BaTbF₆.*** NPD diagrams were recorded on the G4-1 diffractometer, for increasing temperatures in the range 1.4–10 K. No long-range magnetic ordering was observed at $T=1.4$ K, but only a significant modulation of the paramagnetic background, which is the signature of short-range magnetic correlations. These correlations probably arise from weak magnetic interactions between Tb^{4+} ions within the tetramers. The location of this magnetic diffusion signal, close to the (0 1 0) nuclear Bragg position ($d=7.37$ Å), suggest that magnetic interactions may also take place between these tetramers, within the corrugated $[TbF_6]^{2-}$ layers previously described, although its important width indicate a relatively short correlation length.

3.1.3. Magnetic interactions in $BaTbF_6$ fluorides

α and β-$BaTbF_6$ possess the same elements and the same stoichiometry, so that the striking difference in their magnetic behaviour is closely related to their structural characteristics and allows for the investigation of the magnetic interactions involved in these fluoroterbates. Correlation between polyhedral linking and magnetic behaviour of fluoroterbates was previously outlined by a systematic study of their magnetic properties, and led to the notion of "Polyhedra Connection Mode" (PCM) [5]. From this point of view the magnetic behaviours of α and β $BaTbF_6$ are both coherent with the PCM phenomenological rule: the necessity to

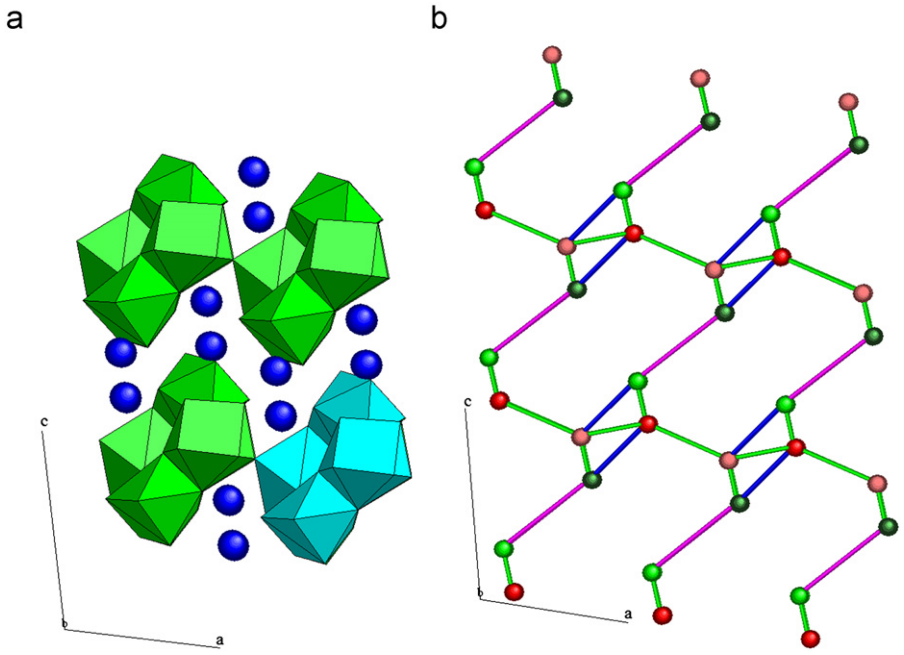

Fig. 3. (a) Crystal structure of α-$BaTbF_6$ viewed along the *b*-axis. Enlightened tetrameric building unit $[Tb_4F_{26}]^{10-}$ in clear blue, Ba^{2+} in cyan. (b): three-dimensional framework formed by Tb^{4+} ions less than 5.76 Å from one another, viewed along the *b*-axis (atoms in green: Tb1, in red: Tb2, in blue, edge-sharing connexion, in green, corner sharing connexion, in purple unconnected Tb^{4+} ions separated by 5.13 Å.). (For interpretation of the references to color in this figure legend, the reader is referred to the web version of this article.)

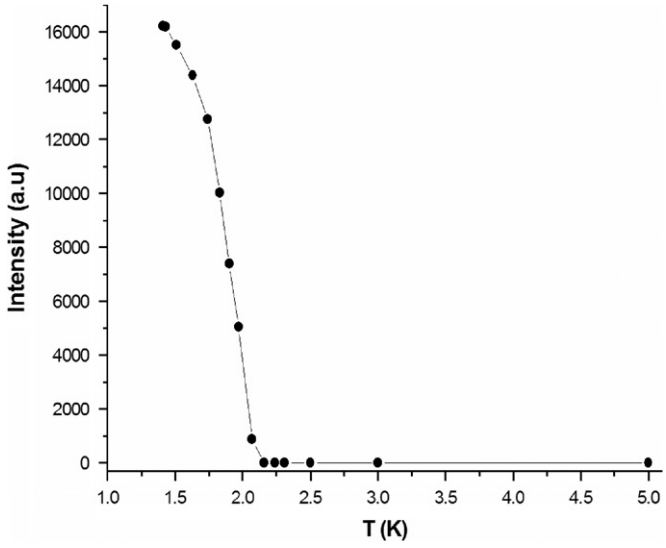

Fig. 4. Thermal variation of the (0 1 1/2) magnetic reflection integrated intensity of β-$BaTbF_6$.

Table 4
Irreducible representations associated to the G_k group (Kovalev's notation [14]).

	h_1	h_4	h_3	h_2	h_{25}	h_{28}	h_{27}	h_{26}
τ_1	1	1	1	1	1	1	1	1
τ_2	1	1	1	1	−1	−1	−1	−1
τ_3	1	1	−1	−1	1	1	−1	−1
τ_4	1	1	−1	−1	−1	−1	1	1
τ_5	1	−1	1	−1	1	−1	1	−1
τ_6	1	−1	1	−1	−1	1	−1	1
τ_7	1	−1	−1	1	1	−1	−1	1
τ_8	1	−1	−1	1	−1	1	1	−1

Table 5
β-$BaTbF_6$ magnetic structure: basis vectors as determined from Bertaut's representation analysis and refined values for the Tb^{4+} magnetic moment components (representation τ_1 from NPD data refinement).

I.R	B.V	Tb^{4+} S_1 at [1/4 0 0] $M_x\ M_y\ M_z$	Tb^{4+} S_2 at [3/4 0 0] $M_x\ M_y\ M_z$	Tb^{4+} S_1	Tb^{4+} S_2
				Refined values (μ_B) $\{M_x\ M_y\ M_z\}$	
τ_1	ψ_1	100	100	M_x=6.68(3)	
τ_2	ψ_2	100	−100	M_x	$-M_x$
τ_3	ψ_3	010	010	M_y	
τ_4	ψ_4	010	0−10	M_y	$-M_y$
τ_5	ψ_7	001	001	M_z	
τ_6	ψ_8	001	00−1	M_z	$-M_z$

have either at least 50% of edges in the connection between terbium polyhedra, or a continuous edge pathway, to observe long range magnetic order at low temperature. These criteria are fulfilled for β-$BaTbF_6$ (infinite chains of 100% edge-connected polyhedra). In the case of α-$BaTbF_6$, the Tb^{4+} polyhedra are only 33.3% edge-connected, and with no infinite edge pathway (connections within a $[Tb_4F_{26}]^{10-}$ tetramer).

In order to investigate the magnetic interactions involved in these compounds, Table 7 recalls the relevant distances and angles for both forms of the $BaTbF_6$ fluoride. Clearly, two types of magnetic interaction can be considered there: magnetic exchange and dipolar ones. Let us examine them both consecutively.

Let us first now examine the case of exchange interactions between neighbouring Tb^{4+} ions, either direct or indirect. Firstly, direct exchange interactions are highly unlikely, considering the large Tb^{4+}–Tb^{4+} distances in both compounds. We shall then focus our interest on indirect exchange, via Tb–F–Tb super-exchange paths, and analyse the Tb–F distances in both $BaTbF_6$ compounds, α and β. In β-$BaTbF_6$, the four Tb–F distances associated to edge-shared polyhedra are identical and equal to 2.28 Å. Something similar is observed for α-$BaTbF_6$, but with less

Table 6
Characteristics of the Rietveld refinement of β-$BaTbF_6$ and $CdTbF_6$ magnetic structures at 1.4 K.

	β-$BaTbF_6$ (magnetic, G4-1)	$CdTbF_6$ (magnetic, G4-1)
System and space group	Orthorhombic *Cmma* (no. 67)	Triclinic, *P*1 (no. 1)
Refined cell parameters	$a=7.756(1)$ Å, $b=11.593(1)$ Å $2c=10.965(1)$ Å $Z=\mathbf{8}$	$a=b=10.348(2)$ Å $c=7.691(2)$ Å
Wavelength	2.4266 Å	2.4266 Å
2θ range/step	8–88° × 0.1	8–88°/0.1
Independent reflections	531	352
Intensity dependent parameters	7	1
Rietveld reliability factor (%)		
R_p	10.0	49.4
R_{wp}	10.9	42.4
R_{Bragg}	4.39	Magnetic pattern only
R_{mag}	1.37	34.1
R_F	4.16	6.56
χ^2	22.0	2.31

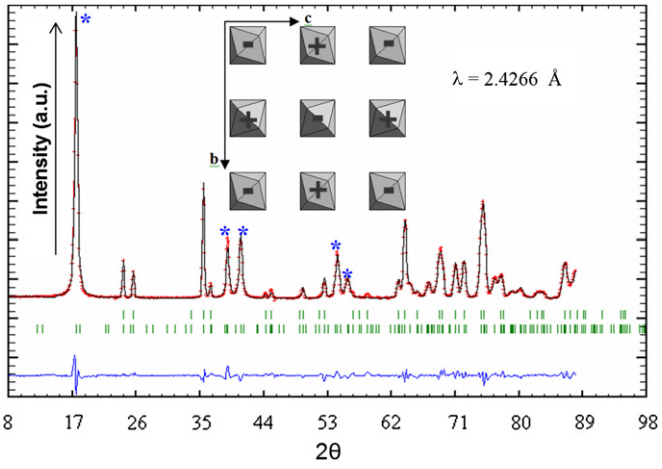

Fig. 5. Rietveld plot of the refinement of the magnetic structure of β-$BaTbF_6$ at 1.4 K. The most intense magnetic reflexions are marked by *. Inset: magnetic structure of β-$BaTbF_6$ viewed along the *a*-axis.

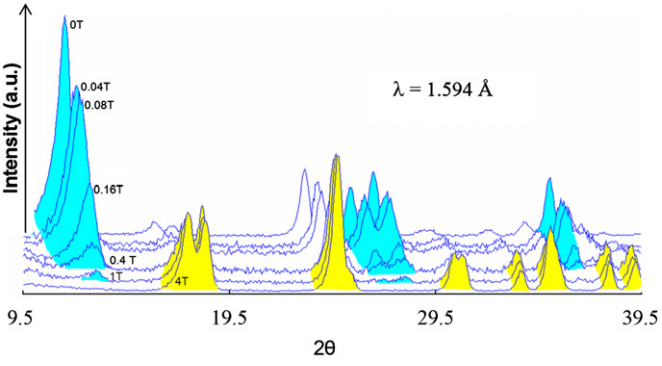

Fig. 6. Evolution of the magnetic diffraction pattern of β-$BaTbF_6$ with a vertical magnetic field (0, 0.04, 0.08, 0.16, 0.4, 1 and 4 T from top to bottom) at 1.4 K.

regular edge-shared polyhedra (two Tb–F distances smaller and two higher than 2.28 Å, with the same mean distance value), and no continuous edge-pathway. Let us also note that the Tb–F

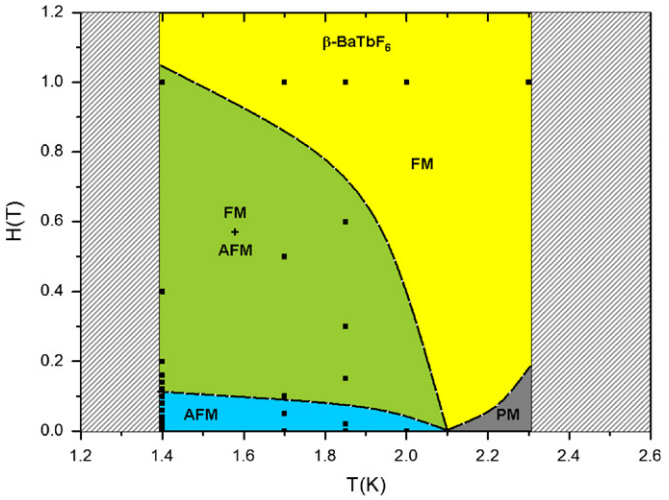

Fig. 7. Tentative magnetic phase diagram for β-$BaTbF_6$. The dashed lines are hypothetical boundaries extrapolated from our experimental observations.

distances corresponding to shared corners in α-$BaTbF_6$, either within the tetrameric unit or between two neighbouring tetramers, are all shorter than or equal to Tb–F distances for edged shared polyhedra in the same compound. From experimentally observed magnetic properties, either in α-$BaTbF_6$ (long-range magnetic order) or β-$BaTbF_6$ (short-range magnetic correlations), the magnetic behaviour of the polymorphic fluoroterbate $BaTbF_6$ is then consistent with the existence of superexchange interactions.

Of course dipolar interaction are always involved in magnetic ordering, and the large distance separating the spin chains in β-$BaTbF_6$ unambiguously indicates that their coupling rely on dipolar interactions. A potential Tb–F – $_{(Ba)}$ – F–Tb super–superexchange coupling should be inexistent considering the already weak superexchange interaction taking place between Tb^{4+} magnetic moments in β-$BaTbF_6$, as suggested by the low ordering temperature: $T_N=2.1$ K. Dipolar interactions couple the spin chains antiferromagnetically and allow for the existence of a long range, three-dimensional, magnetic order. The easy reversal of one of the magnetic sublattices of antiferromagnetic β-$BaTbF_6$ by an external magnetic field shows their relative weakness, yielding the observed metamagnetic behaviour. Furthermore, dipolar energy calculations show that in β-$BaTbF_6$, ferromagnetic chains are more stable with magnetic moments oriented along the *a*-axis (−1265 mK (*a*-axis) vs +560 mK (*b*-axis) and +700 mK (*c*-axis)), which is the orientation actually observed in this work. However the striking difference between the magnetic behaviours of α and β forms of $BaTbF_6$ requires the consideration of superexchange interactions to be explained.

3.2. *$CaTbF_6$ and $CdTbF_6$ fluorides*

3.2.1. *Nuclear structure*

The room temperature crystal structures of $CaTbF_6$ and $CdTbF_6$ have been determined and presented in details in a previous study [2], the results of which were used in the present work. The anti-$KSbF_6$ structure of these compounds is represented in Fig. 1. However neutron diffraction has revealed the polymorphic behaviour of $CaTbF_6$.

On cooling the sample on the G4-1 diffractometer, a first order phase transition was observed in $CaTbF_6$. The transition occurs around 220 K on cooling and around 250 K on heating. Attempts to determine the unit cell were unsuccessful, and thus the low temperature crystal-structure could not be determined at the moment.

Table 7
Topological data for α and β-$BaTbF_6$ at 300 K.

Shared edges			Shared corners			Others
Distances (Å)		Angle (deg.)	Distances (Å)		Angle (deg.)	Distances (Å)
Tb–Tb	Tb–F	Tb–F–Tb	Tb–Tb	Tb–F	Tb–F–Tb	Tb–Tb
α-$BaTbF_6$						
3.83	*Tb1*	*Tb1–F–Tb2*	*Tb1–Tb2*	*Tb1*	*Tb1–F–Tb2*	*Tb1–Tb2*
	2.17/2.44	116.2°	4.26	2.18	161.4	5.07–5.61
	Tb2	*Tb2–F–Tb1*	*Tb2–Tb2*	*Tb2*	*Tb2–F–Tb2*	*Tb1–Tb1*
	2.17/2.34	112.2°	4.36	2.13	180.0 × 2	5.13–5.35
			Tb2–Tb2	2.18		
			4.56	2.28		
β-$BaTbF_6$						
3.88	2.27	117.4°	–	–	–	5.52
						5.76

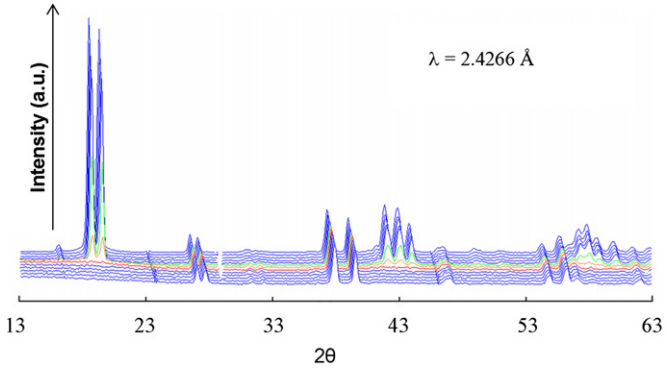

Fig. 8. Evolution of $CaTbF_6$ neutron diffraction pattern between 5 K (front pattern) and 1.4 K (rear pattern).

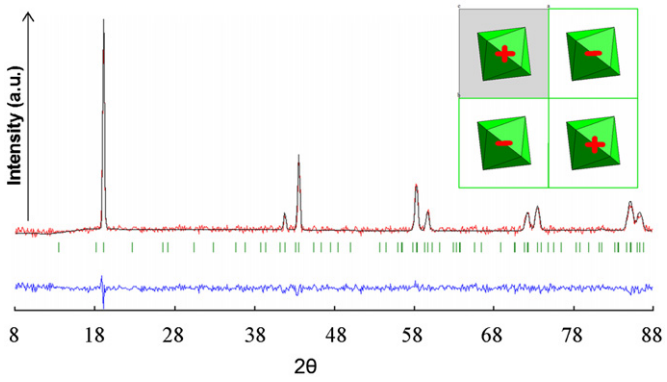

Fig. 9. Rietveld plot of the difference pattern (1.83 K–4.13 K) refinement of the magnetic structure of $CdTbF_6$. Inset: magnetic structure of $CdTbF_6$ viewed along the *c*-axis.

Given the important absorption cross-section of Cadmium (2520 barns), which necessitates long counting times to obtain a good statistic, NDP have been recorded at room and low temperatures ($T<5$ K) only for this sample. Comparison of these diagrams suggests a small modification of the crystal structure (two small additional contribution at $2\theta=60°$ and 77°), but no satisfying structural hypothesis could be elaborated from our experimental data.

3.2.2. Magnetic studies

NDP recorded at low temperature on $CaTbF_6$, and also on $CdTbF_6$ revealed that these two fluoroterbates exhibit long range magnetic order around 2.15 K ($CaTbF_6$, Fig. 8) and 2.70 K ($CdTbF_6$). In both cases the observation of purely magnetic contributions in the NDP accounts for the onset of an antiferromagnetic order. Since the crystal structure of the low-temperature form of $CaTbF_6$ remains unknown, the determination of the magnetic structure of $CaTbF_6$ could not be undertaken.

In the case of $CdTbF_6$, however, considering that the structural rearrangement is minor and does not affect the cationic sublattice, phenomenological considerations allowed us to determine the magnetic structure of this tetravalent terbium fluoride.

First, the magnetic diagram was obtained in form of the difference diagram (1.83–4.13 K). This revealed a quite simple magnetic diffraction pattern, but since the structural distortion was not elucidated, the actual symmetry of the material remains unknown and thus representational analysis could not be performed.

However, the $[TbF_6]^{2-}$ chains arranged in a tetragonal packing in $CdTbF_6$ crystal structure may be compared to the corrugated chains (edge-sharing antiprisms) observed in the M_2TbF_6 (M=Li, K, Rb) series of terbium fluorides [6]. In these latter compounds, Tb^{4+} magnetic moments are coupled ferromagnetically within the chains, the interchain interactions being antiferromagnetic. By analogy, we envisaged for $CdTbF_6$ a magnetic structure built of ferromagnetic $[TbF_6]^{2-}$ chains coupled antiferromagnetically.

Since there are two Tb^{4+} ions in the nuclear unit cell, located at (1/2 1/2 1/4) and (1/2 1/2 3/4), such a magnetic structure, as the chains expand along the z direction, require a $\vec{k}=(1/2\ \ 1/2\ \ 0)$ propagation vector, i.e. a fourfold magnetic cell as compared to the nuclear cell.

The simulated NDP corresponding to this hypothesis revealed a perfect agreement with the observed magnetic pattern (Fig. 9). Rietveld refinement of this hypothesis, using the difference pattern previously mentioned, confirmed this magnetic structure, with a refined magnetic moment of 6.5 μ_B for the Tb^{4+} ion (theoretical value: 7.0 μ_B).

Table 6 gathers the details of this refinement, for which the elevated values of R_p, R_{wp} et R_{exp} arise from the weak signal to noise ratio of our data, due to the presence of cadmium in our sample.

3.3. $SrTbF_6$

3.3.1. Nuclear structure

Although $SrTbF_6$ was one of the first tetravalent terbium fluorides synthesised, its crystal structure has never been investigated. Burns et al. [9] reported $SrTbF_6$ to be isotypic to $RbPaF_6$, i.e. to β-$BaTbF_6$, but our attempts to fit the neutron diffraction

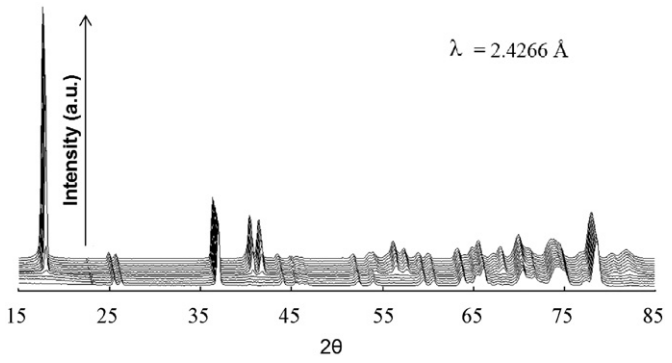

Fig. 10. Evolution of the neutron diffraction pattern of $SrTbF_6$ between 5 K (front pattern) and 1.4 K (rear pattern).

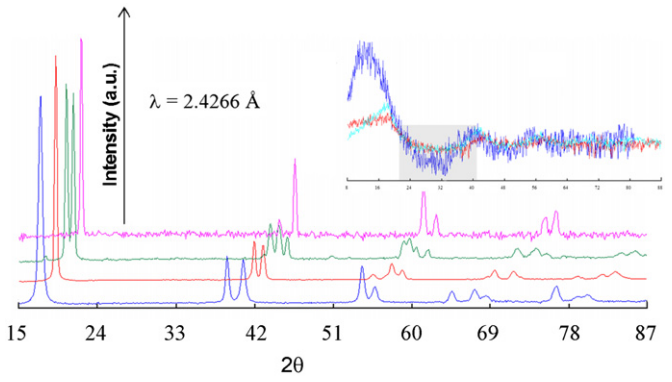

Fig. 11. Magnetic diffraction pattern of β-$BaTbF_6$ (front), $SrTbF_6$, $CaTbF_6$ and $CdTbF_6$ (rear) at 1.4 K. Inset: diffusion signal ascribable to short range magnetic correlations detected in β-$BaTbF_6$ (blue), $SrTbF_6$ (red) and $CaTbF_6$ (cyan). Grey rectangle: 1D signal. (For interpretation of the references to color in this figure legend, the reader is referred to the web version of this article.)

data using this hypothesis were unsuccessful, as several significant contributions were not simulated.

Upon cooling, in order to study the magnetic properties of $SrTbF_6$ at low temperature, a nuclear phase transition was observed around 210–220 K. Similarly to the case of $CaTbF_6$, the unit cell could not be determined from our diffraction data.

3.3.2. *Magnetic studies*

NDP recorded between 1.40 and 5 K revealed the appearance of a long range antiferromagnetic order in $SrTbF_6$ below 2.6 K (Fig. 10). Although the magnetic diffraction pattern of $SrTbF_6$ is relatively simple, the magnetic structure could not be solved given the absence of structural model for its low temperature phase.

3.4. *Magnetic interactions in $MTbF_6$ tetravalent terbium fluorides*

Since all the magnetically ordered fluoroterbates of this study exhibit a crystal-structure built of $[TbF_6]^{2-}$ chains, and thus a pronounced one-dimensional character concerning their magnetic properties, it is worth comparing the magnetic diffraction patterns of the compounds.

Fig. 11 shows that the sequence of magnetic Bragg peaks is similar in the whole family, the splitting of some contributions, particularly in the case of $CaTbF_6$, being much likely related to a structural transition, observed around 220 K in this compound. The inset of Fig. 11 displays the pre-ordering magnetic diffusion signals observed in this family. These signals are identical for all representatives, and some of their features (signal around 32° (2θ)) are characteristics of one-dimensional systems, as previously exemplified during the study of Li_2TbF_6 fluoroterbate, the structure of which is also based on $[TbF_6]^{2-}$ chains.

Thus, from the similarities of their magnetic behaviour, it is likely that the magnetic order in these compounds relies on the establishment of superexchange interactions, as we demonstrated from the study of the polymorphic fluoroterbate $BaTbF_6$.

4. Conclusion

In this work the magnetic behaviour of the $MTbF_6$ fluorides (M=Ca, Sr, (α/β)-Ba, Cd) was investigated by means of neutron powder diffraction. A magnetic order was observed in all compounds except α-$BaTbF_6$, the crystal structure of which was investigated by high-resolution neutron powder diffraction.

The magnetic structures of $CdTbF_6$ and β-$BaTbF_6$ were determined from phenomenological considerations, consistently with Bertaut's representational analysis in the case of β-$BaTbF_6$. A neutron diffraction study under magnetic field emphasised the metamagnetic behaviour of β-$BaTbF_6$.

In previous works, the study of fluoroterbates with various dimensionalities [5] correlated the ordering temperature to the Polyhedra Connection Mode and suggested that non-dipolar interaction may occur in tetravalent terbium fluorides.

The analysis of the magnetic behaviour of the polymorphic fluoroterbate $BaTbF_6$, on the basis of topological parameters, reveals the existence of superexchange interactions. These magnetic interactions are likely to be involved in the other member of the $MTbF_6$ (M=Ca, Sr, (α/β)-Ba, Cd) family, all built of $[TbF_6]^{2-}$ chains, as suggested by their similar magnetic behaviours. This work confirm the fact that dipolar interactions only are not sufficient to explain the magnetic order in one-dimensional fluoroterbates, as was suggested by the study of M'_2TbF_6 (M'=Li, K, Rb) fluorides [6], and demonstrate the existence of superexchange interactions, promoted by Tb^{4+} polyhedra edge sharing.

To complete these studies, the magnetic properties of tetravalent terbium fluorides with other dimensionalities for their polyhedral framework (for example two-dimensional matrices) will be presented in a future article.

The study of the magnetic properties of fluoroterbates, initially engaged after the observation of a favoured capacity for the Tb^{4+} ion to assume eight-coordination, will also be worth of interest concerning the recently discovered fluoroterbates in which the Tb^{4+} ion adopt a seven-coordination [15]. The topological differences associated with such an environment could allow for a better understanding of the magnetic ordering in tetravalent terbium fluoride.

References

[1] Y. Laligant, Bail A. Le, G. Ferey, D. Avignant, J.C. Cousseins, Eur. J. Solid State Inorg. Chem. 25 (5–6) (1989) 551–563.
[2] M. Josse, M. Dubois, M. El-Ghozzi, J. Cellier, D. Avignant, Acta Cryst. B61 (2005) 1–10.
[3] E. Largeau, M. El-Ghozzi, D. Avignant, M. Guillot, F. Bouree, G. Andre, A. Cousson, J. Magn. Magn. Mater. 261 (1–2) (2003) 93–104.
[4] M. Josse, University Thesis, Blaise Pascal University, Clermont-Ferrand, 2003.
[5] M. Josse, M. El-Ghozzi, M. Dubois, D. Avignant, G. André, F. Bourée, Physica B 350 (1–3 Suppl. 1) (2004) E43–E45.
[6] M. Josse, M. El-Ghozzi, D. Avignant, G. André, F. Bourée, J. Solid State Chem. 180 (5) (2007) 1623–1635.
[7] E. Largeau, V. Gaumet, M. El-Ghozzi, D. Avignant, J.C. Cousseins, J. Mater. Chem. 7 (9) (1997) 1881–1885.
[8] E. Largeau, V. Gaumet, M. El-Ghozzi, J. Metin, D. Avignant, Acta Cryst. C53 (1997) 530–532.

[9] J.H. Burns, H.A. Levy, O. Lewin Keller Jr., Acta Cryst. B24 (1968) 1675–1680.
[10] T. Roisnel, J. Rodriguez-Carvajal, M. Pinot, G. André, F. Bourée, Mater. Sci. Forum 245 (1994) 166–169.
[11] J. Rodriguez-Carvajal, Abstracts of the Satellite Meeting on Powder Diffraction of the XV Congress of the IUCr, Toulouse, France, 1991, pp. 127.
[12] E.F. Bertaut, J. Phys. 39 (1978) 1331–1348 (and references therein).
[13] E.F. Bertaut, Acta Cryst. A24 (1968) 217–231.
[14] O.V. Kovalev, Representations of the Crystallographic Space Groups: Irreducible Representations and Corepresentations, 2nd Edition, Gordon and Breach Science Publishers, Switzerland, 1993.
[15] L. Meddar, M. El-Ghozzi, D. Avignant, Z. Anorg. Allg. Chem. 634 (2008) 565–570.